Electronic Supplementary Information

Experimental section

Materials: Iron (III) nitrate nonahydrate ($Fe(NO_3)_3{\cdot}9H_2O$), ruthenium oxide (RuO_2), and Nafion (5 wt.%) were acquired from Aladdin Reagent (Shanghai, China). Nitrate hexahydrate ($Ni(NO_3)_2{\cdot}6H_2O$), ammonium molybdate tetrahydrate ($(NH_4)_6Mo_7O_{24}{\cdot}4H_2O$), sodium hydroxide (NaOH), potassium hydroxide (KOH), sodium chloride (NaCl), sodium monophosphate (NaH_2PO_2), disodium phosphate anhydrous (Na_2HPO_4), potassium phosphate monobasic (KH_2PO_4), ethylenediaminetetraacetic acid disodium (EDTA-2Na), commercial Pt/C (20 wt.%), tetramethylammonium hydroxide (TMAOH), N, N-diethyl-p-phenylenediamine (DPD) was obtained from Shanghai Maclin Biochemical Technology Co., Ltd. Ethanol (C_2H_5OH), potassium permanganate ($KMnO_4$), sulfuric acid (H_2SO_4), and hydrochloric acid (HCl) were purchased from Beijing Chemical Reagent Co., Ltd. (Beijing, China). Natural seawater was collected from Qingdao (Shandong, China), and most of the magnesium and calcium salts were removed by adding Na_2CO_3 to the natural seawater before use. Ni foam (NF) was purchased from Qingyuan Metal Materials Co., Ltd (Xingtai, China). All reagents were utilized as received, without additional purification. Throughout all experiments, water was purified through a Millipore system.

Preparation of $NiMoO_4$/NF: In a typical synthesis process, 0.35 g $(NH_4)_6Mo_7O_{24}{\cdot}4H_2O$ and 0.37 g $Ni(NO_3)_2{\cdot}6H_2O$ were mixed with 30 mL of deionized water and stirred for 20 minutes at room temperature to obtain a precursor solution. NF (2.0×3.0 cm^2) was sonicated in HCl, ethanol, and water for 15 min, respectively. The prepared NF was put into a Teflon-lined autoclave along with the abovementioned precursor solution. The autoclave was sealed and maintained at 150 °C for 6 h in an oven and then cooled down to room temperature naturally. Then, the $NiMoO_4$/NF was taken out and thoroughly washed with deionized water and ethanol several times, then dried at 60 °C for 2 h.

Preparation of FeNiP/MoO_x/$NiMoO_4$/NF: A piece of cleaning $NiMoO_4$/NF (2.0 ×

2.0 cm^2) was immersed in 0.1 M $Fe(NO_3)_3 \cdot 9H_2O$ solution for 5 min and dried at 60 °C. Then Fe-$NiMoO_4$/NF was located downstream of a tubular furnace, and 1.0 g NaH_2PO_2 was upstream in the atmosphere of Ar gas flow. The tubular furnace was gradually heated to 350 °C at a rate of 2 °C min^{-1}, maintaining this temperature for 3 h. After the furnace naturally cooled down to room temperature, the obtained black FeNiP/MoO_x/$NiMoO_4$/NF sample was taken out.

Preparation of NiP/MoO_x/$NiMoO_4$/NF: The same technique was used to obtain the NiP/MoO_x/$NiMoO_4$/NF catalyst as FeNiP/MoO_x/$NiMoO_4$/NF, but without the $Fe(NO_3)_3 \cdot 9H_2O$ immersing process.

Preparation of RuO_2/NF and Pt/C/NF: 5 mg RuO_2 (or 20 wt.% Pt/C) was added into a solution containing 30 μL of Nafion, 485 μL of ethanol, and 485 μL of deionized water with the aid of ultrasonication (30 min) to form a homogeneous ink (5 mg mL^{-1}). 300 μL of catalyst ink was dropped onto a piece of cleaned NF (0.5 × 0.5 cm^2) with a loading mass of 1.5 mg.

Preparation of alkaline seawater: Firstly, 6.8 g of Na_2CO_3 was added to 1 L of natural seawater under stirring conditions and left to stand for half a day before being pumped. Then, 1 M KOH was added to 1 L of filtrate and centrifuged after standing overnight to obtain alkaline seawater.

Characterizations: XRD data were acquired via X-ray diffraction (XRD, Philip D8) with Cu Kα source (λ = 1.54056 Å). Raman spectroscopy was recorded on the Lab RAM HR Evolution confocal microscope with a 532 nm laser. Scanning electron microscopy (SEM, ZISS 300) equipped with an energy dispersive X-ray (EDX) facility, transmission electron microscopy (TEM, JEM-F200, JEOL Ltd.), and X-ray photoelectron spectroscopy (XPS, ESCALAB 250 Xi) were utilized to research the morphology and compositions of samples. Absorbance data were acquired on a UV-vis spectrophotometer (Shimadzu UV-2700).

Electrochemical measurements: All electrochemical tests were performed using a three-electrode system on a CHI 660E electrochemical workstation. The prepared

$FeNiP/MoO_x/NiMoO_4/NF$ served as the working electrode (comprising an area of 0.5 × 0.5 cm^2), while a graphite rod acted as the counter electrode, and a Hg/HgO electrode was employed as the reference electrode. Oxygen evolution reaction (OER) activity tests were conducted under three alkaline conditions, including alkaline freshwater (1 M KOH), alkaline simulated seawater (1 M KOH + 0.5 M NaCl), and alkaline seawater (1 M KOH + seawater), at a pH of approximately 14. In accordance with the Nernst equation ($E_{RHE} = E_{Hg/HgO} + 0.059 \times pH + 0.098$ V), all potentials reported in this study were expressed relative to the reversible hydrogen electrode (RHE). Linear sweep voltammetry (LSV) curves were measured within the range from 0 to 1.4 V at a scan rate of 5 mV s^{-1}. The Tafel slope was calculated by the Tafel formula ($\eta = b \log j + a$), where η is the overpotential, b is the Tafel slope (mV dec^{-1}), and j is the current density (mA cm^{-2}). Electrochemical impedance spectroscopy (EIS) was performed in the range of 10^5 to 0.01 Hz with an amplitude of 5 mV in 1 M KOH. The capacitance of the double layer (C_{dl}) was determined in 1 M KOH via cyclic voltammetry (CV) at different scan rates ranging from 20 to 120 mV s^{-1}. The iR-compensated potential was calculated by correcting for the solution resistance, using the equation $E_{corr.} = E - iR$, where E represents the original potential, R is the solution resistance, i is the corresponding current, and $E_{corr.}$ denotes the iR-compensated potential.

TOF calculation: The TOF is evaluated based on the concentration of active sites and calculated using: $TOF = Aj/4Fm$. Here, A represents the geometric area of the test electrode, j denotes current density, 4 signifies the moles of electron consumption for one mole of O_2 evolution, F is the Faradic constant (96,485 C mol^{-1}), and m represents the number of active sites (mol). The value of m can be determined from the linear relationship between the oxidation peak currents and scan rate using the equation: $Slope = n^2F^2m/4RT$ (Figure S15), with n assuming an electron transfer number of 1 for a single-electron process involving the oxidation of the metal center in the catalyst. The TOF test was performed three times, and we took the middle value for subsequent calculations.

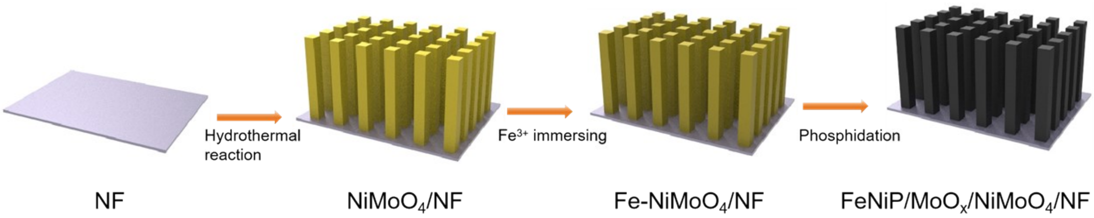

Fig. S1. Schematic diagram of the fabrication process of FeNiP/MoO_x/$NiMoO_4$/NF.

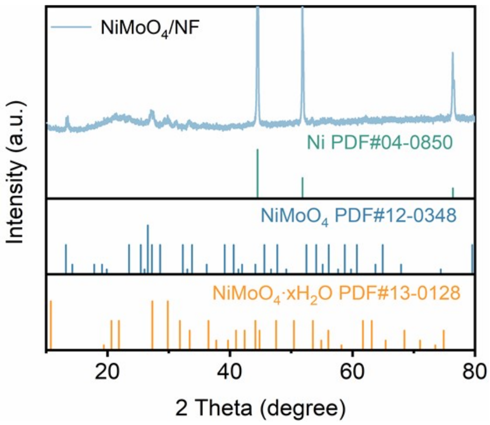

Fig. S2. XRD pattern of $NiMoO_4$/NF.

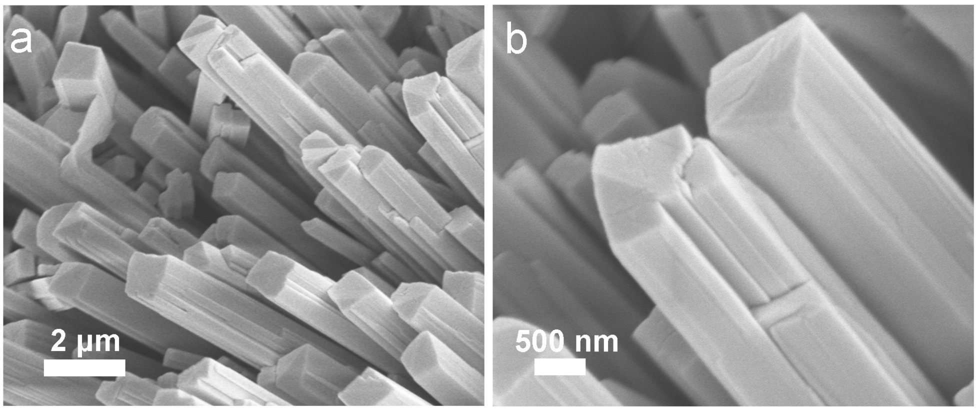

Fig. S3. (a) Low- and (b) high-magnification SEM images of $NiMoO_4$/NF.

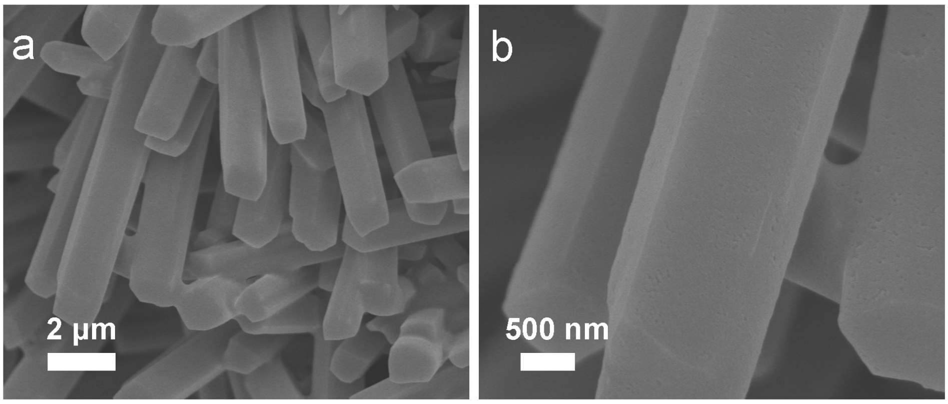

Fig. S4. (a) Low- and (b) high-magnification SEM images of NiP/MoO_x/$NiMoO_4$/NF.

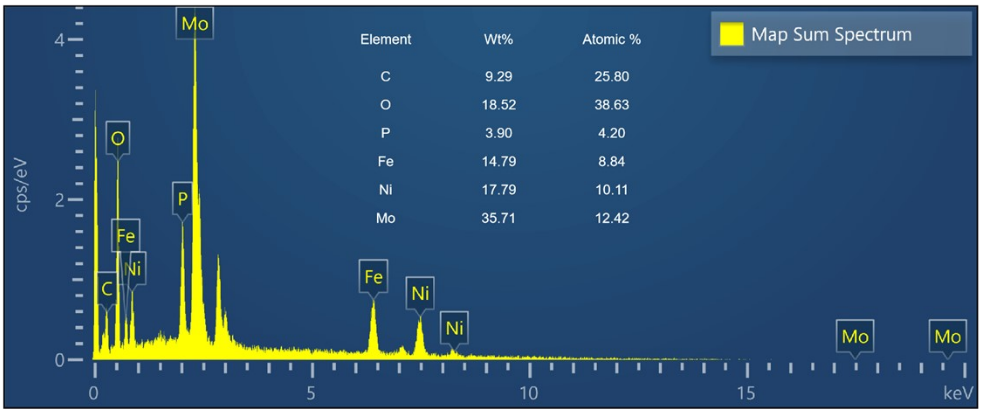

Element	Wt%	Atomic %
C	9.29	25.80
O	18.52	38.63
P	3.90	4.20
Fe	14.79	8.84
Ni	17.79	10.11
Mo	35.71	12.42

Fig. S5. EDX spectrum of FeNiP/MoO_x/$NiMoO_4$.

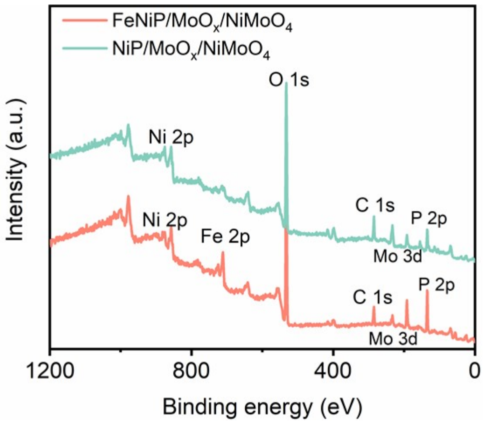

Fig. S6. XPS Survey spectra for FeNiP/MoO_x/$NiMoO_4$ and NiP/MoO_x/$NiMoO_4$.

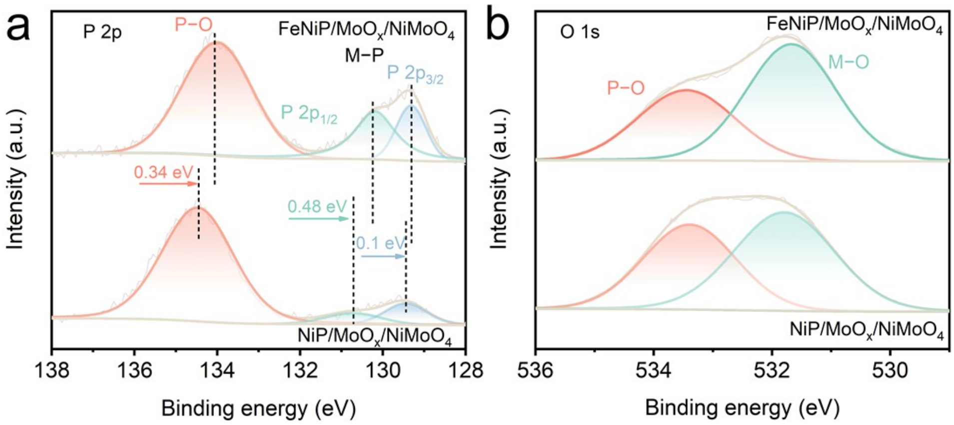

Fig. S7. High-resolution XPS spectra for FeNiP/MoO$_x$/NiMoO$_4$ and NiP/MoO$_x$/NiMoO$_4$ in the (a) P 2p and (b) O 1s regions.

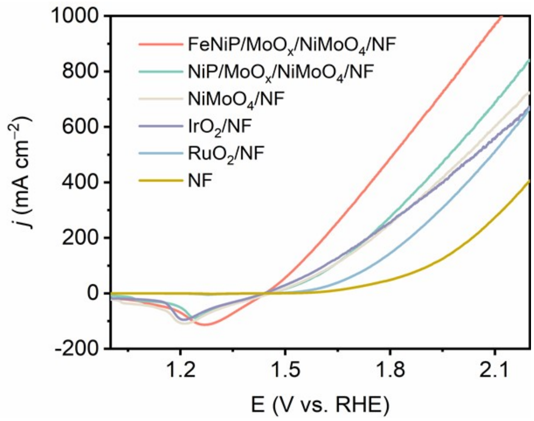

Fig. S8. LSV curves of FeNiP/MoO$_x$/NiMoO$_4$/NF, NiP/MoO$_x$/NiMoO$_4$/NF, NiMoO$_4$/NF, IrO$_2$/NF, RuO$_2$/NF, and NF in 1 M KOH without iR compensation.

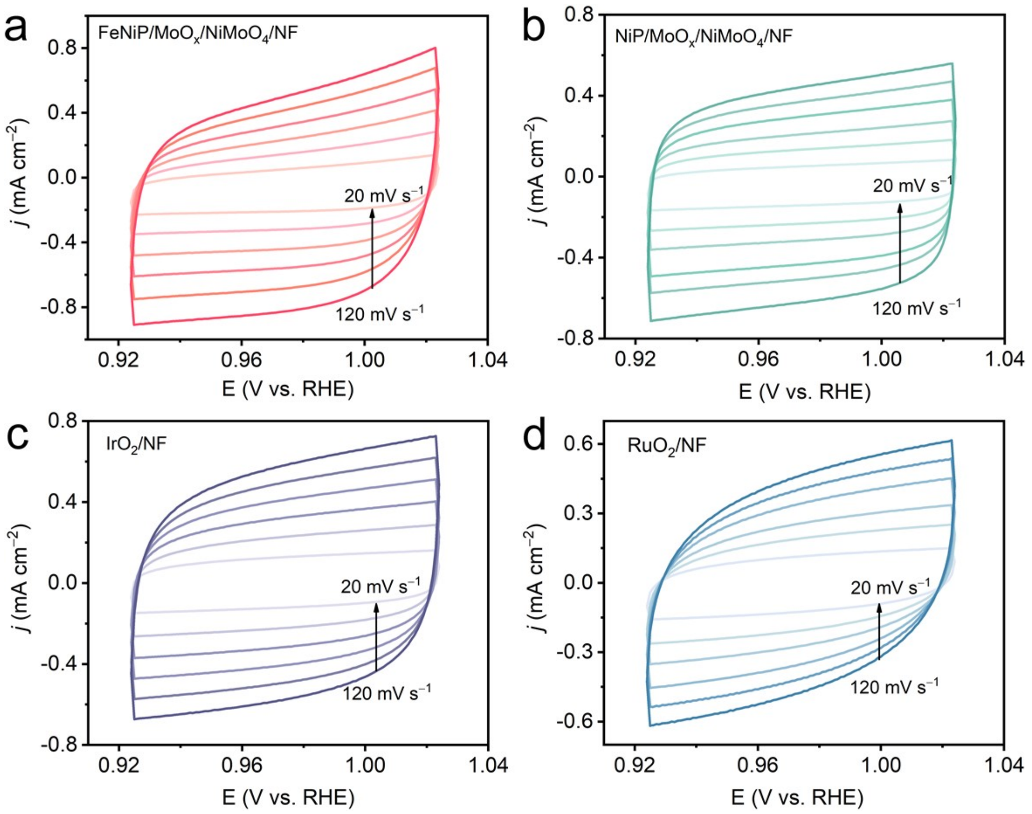

Fig. S9. CV curves of (a) FeNiP/MoO_x/$NiMoO_4$/NF, (b) NiP/MoO_x/$NiMoO_4$/NF, (c) IrO_2/NF, and (d) RuO_2/NF in non-Faradaic region at different scan rates from 20−120 mV s^{-1} in 1 M KOH.

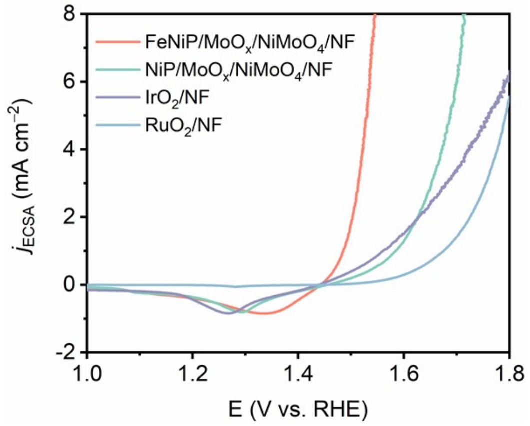

Fig. S10. LSV curves normalized by the electrochemical active surface area in 1 M KOH for FeNiP/MoO$_x$/NiMoO$_4$/NF, NiP/MoO$_x$/NiMoO$_4$/NF, IrO$_2$/NF, and RuO$_2$/NF.

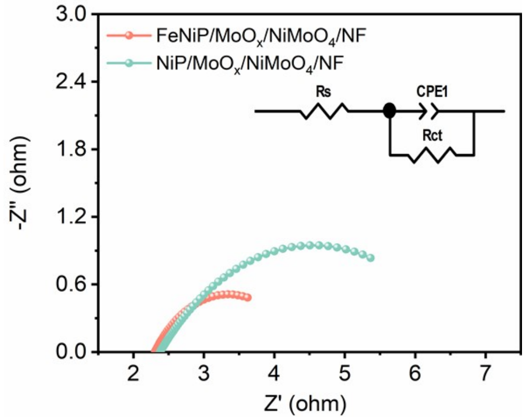

Fig. S11. Nyquist plots of FeNiP/MoO$_x$/NiMoO$_4$/NF and NiP/MoO$_x$/NiMoO$_4$/NF in 1 M KOH.

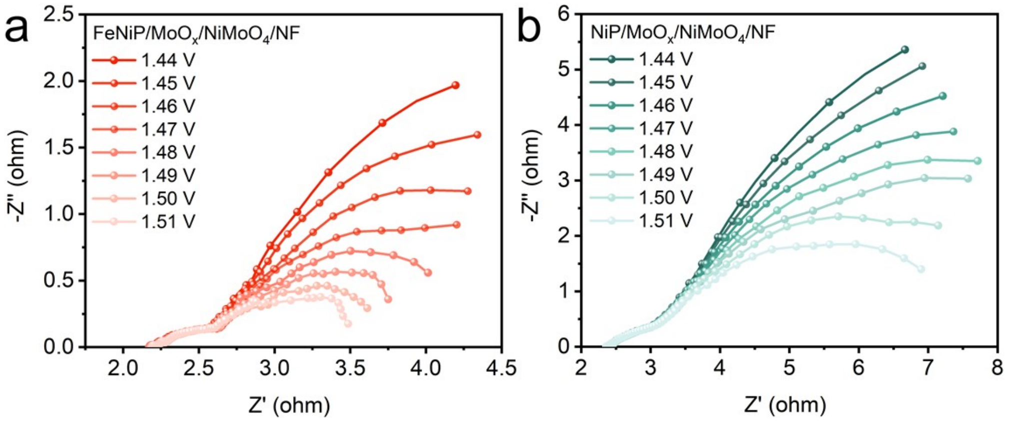

Fig. S12. Operando Nyquist plots of (a) FeNiP/MoO$_x$/NiMoO$_4$/NF and (b) NiP/MoO$_x$/NiMoO$_4$/NF at different potentials in 1 M KOH.

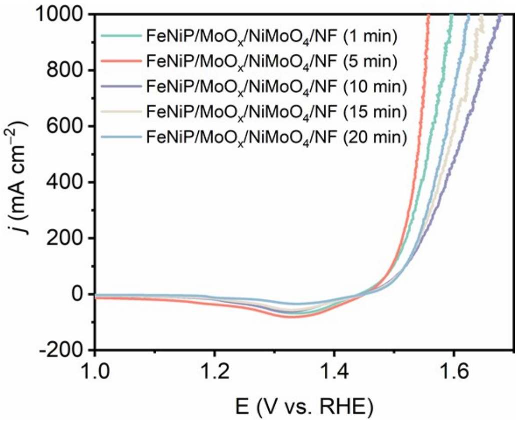

Fig. S13. LSV curves of FeNiP/MoO$_x$/NiMoO$_4$/NF with different immersion time in 1 M KOH + seawater.

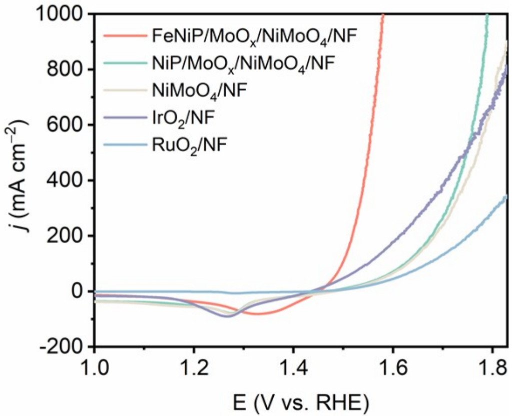

Fig. S14. LSV curves of FeNiP/MoO$_x$/NiMoO$_4$/NF, NiP/MoO$_x$/NiMoO$_4$/NF, NiMoO$_4$/NF, IrO$_2$/NF, and RuO$_2$/NF in 1 M KOH + seawater.

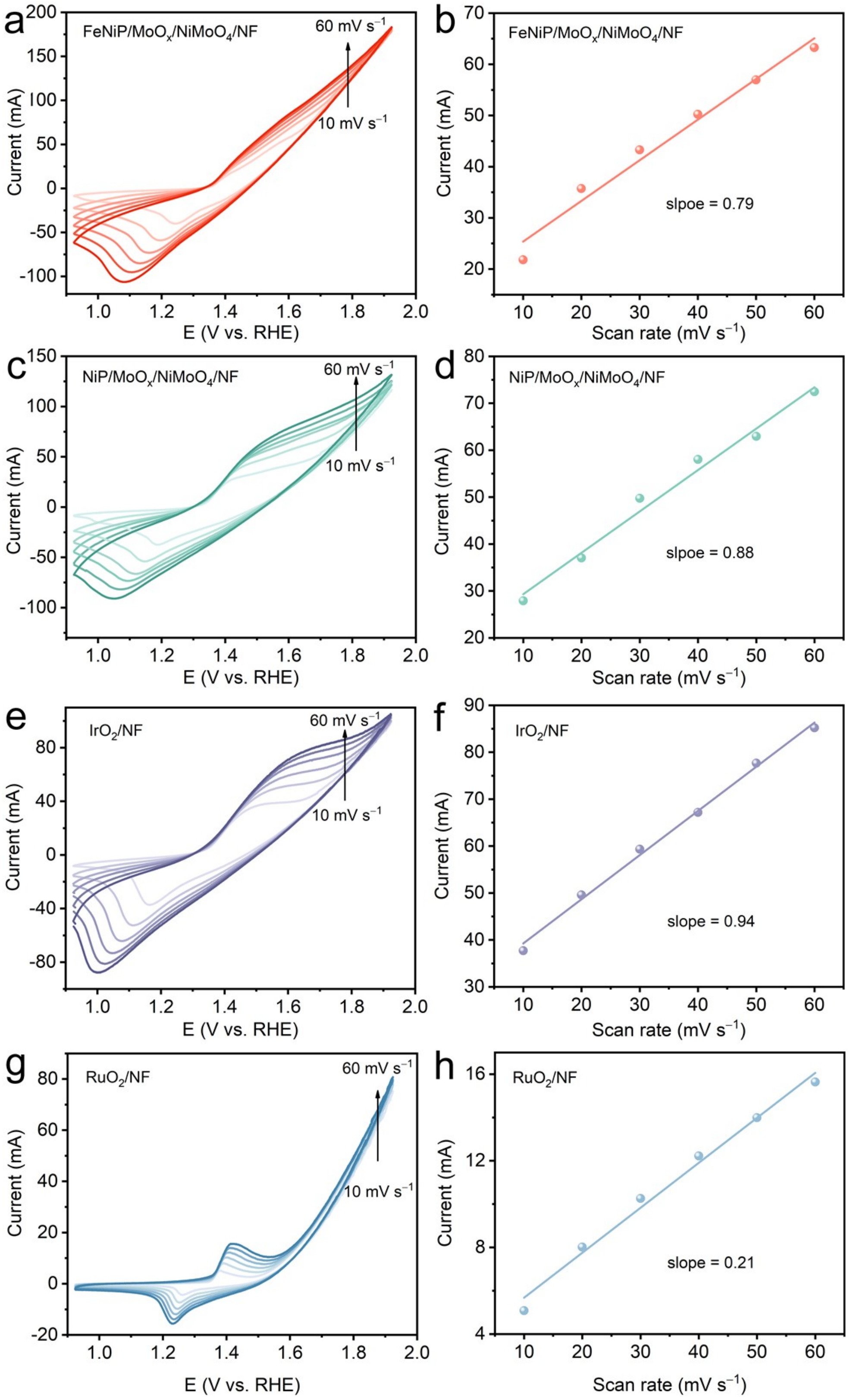

Fig. S15. CV curves for (a) FeNiP/MoO$_x$/NiMoO$_4$/NF, (c) NiP/MoO$_x$/NiMoO$_4$/NF, (e) IrO$_2$/NF, and (g) RuO$_2$/NF at different scan rates increasing from 10 to 60 mV s^{-1} in 1 M KOH + seawater. Oxidation current versus the scan rate plots for (b) FeNiP/MoO$_x$/NiMoO$_4$/NF, (d) NiP/MoO$_x$/NiMoO$_4$/NF, (f) IrO$_2$/NF, and (h) RuO$_2$/NF.

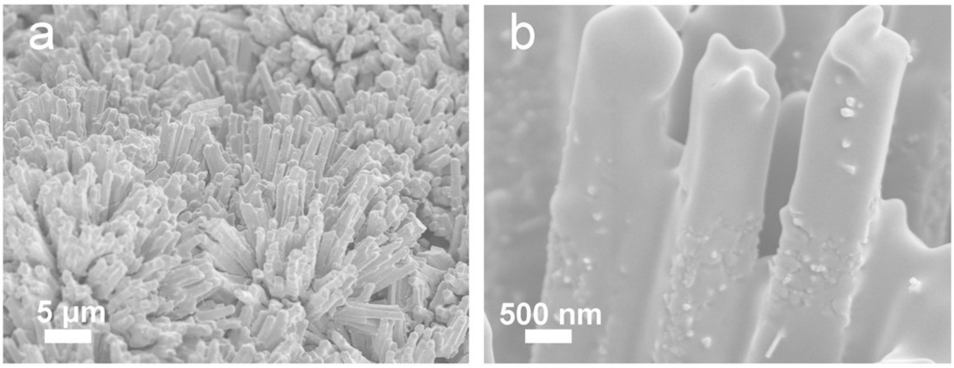

Fig. S16. (a) Low- and (b) high-magnification SEM images of FeNiP/MoO_x/$NiMoO_4$/NF after stability test.

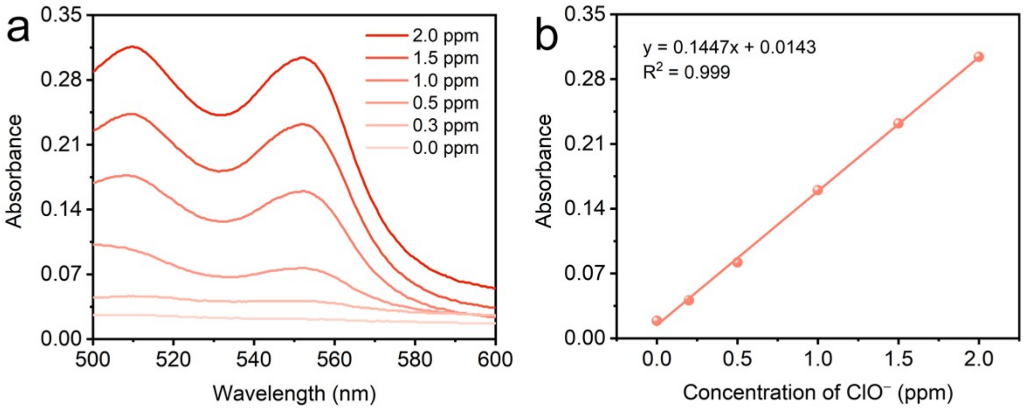

Fig. S17. (a) UV-vis absorption spectra of various active chlorine concentrations and (b) the corresponding linear fit.

Table S1. EIS parameters of the samples.

Catalysts	R_s/Ω	R_{ct}/Ω
$FeNiP/MoO_x/NiMoO_4/NF$	2.28	6.97
$NiP/MoO_x/NiMoO_4/NF$	2.41	9.50

R_s: solution resistance.

R_{ct}: charge transfer resistance.

Table S2. Ion compositions of the natural seawater (before the seawater alkalization) and alkaline seawater (after the seawater alkalization) used in this work.

Species	Conc. [mg L^{-1}] for natural seawater	Conc. [mg L^{-1}] for alkaline seawater
Mg^{2+}	1035.46	0.54
Ca^{2+}	496.38	6.69

Notes**:** The seawater was collected from Huangdao district, Qingdao city, China. The pH value for natural seawater was around 7.85, and the pH for alkaline seawater was around 13.95.

Table S3. Comparison of the OER performance of FeNiP/MoO_x/$NiMoO_4$/NF with other reported seawater OER electrocatalysts.

Catalyst	Electrolyte	η_{1000} (mV)	Time (h)	Ref.
FeNiP/MoO_x/$NiMoO_4$/NF	**1 M KOH + seawater**	**349**	**500 h@1000 mA cm^{-2}**	**This work**
Ni_3S_2/Fe-NiP_x/NF	1 M KOH + seawater	351	30 h@200 mA cm^{-2}	1
Mn-doped Ni_2P/Fe_2P	1 M KOH + seawater	358	200 h@500 mA cm^{-2}	2
Ni_2P@$NiMoO_4$/NF	1 M KOH + seawater	370	500 h@1000 mA cm^{-2}	3
F-$FeCoP_v$@IF	1 M KOH + seawater	370	100 h@100 mA cm^{-2}	4
B, Fe-CoP/NF	1 M KOH + seawater	376	200 h@100 mA cm^{-2}	5
Mo-NiFeP/NIF	1 M KOH + seawater	390	20 h@500 mA cm^{-2}	6
NiFe-MOF@Ni_2P/$Ni(OH)_2$/NF	1 M KOH + seawater	394	120 h@500 mA cm^{-2}	7
Mn-FeP_v/IF	1 M KOH + seawater	395	45 h@100 mA cm^{-2}	8
NiMoN@NiFeN/NF	1 M KOH + seawater	398	100 h@500 mA cm^{-2}	9
Fe-NiO/MoO_2/NF	1 M KOH + seawater	399	50 h@100 mA cm^{-2}	10
Fe-NiS/NF	1 M KOH + seawater	420	25 h@500 mA cm^{-2}	11
Ni_2P-Fe_2P/NF	1 M KOH + seawater	431	24 h@500 mA cm^{-2}	12
R-CoNiPS/NF	1 M KOH + seawater	440	200 h@500 mA cm^{-2}	13
S-Ni/Fe(OOH)	1 M KOH + seawater	462	100 h@500 mA cm^{-2}	14
Ru-FeP_4/IF	1 M KOH + seawater	520	24 h@100 mA cm^{-2}	15

Table S4. Element analysis of FeNiP/MoO_x/$NiMoO_4$/NF and $NiMoO_4$/NF after stability test by ICP-OES.

Catalysts	Element	Element concentration (mg/L)
FeNiP/MoO_x/$NiMoO_4$/NF	Mo	37.09
	Fe	0.038
	P	15.68
$NiMoO_4$/NF	Mo	95.17

References

1 X. Luo, P. Ji, P. Wang, X. Tan, L. Chen and S. Mu, *Adv. Sci.*, 2022, **9**, 2104846.

2 Y. Luo, P. Wang, G. Zhang, S. Wu, Z. Chen, H. Ranganathan, S. Sun and Z. Shi, *Chem. Eng. J.*, 2023, **454**, 140061.

3 X. Guo, X. He, X. Liu, S. Sun, H. Sun, K. Dong, T. Li, Y. Yao, T. Xie, D. Zheng, Y. Luo, J. Chen, Q. Liu, L. Li, W. Chu, Z. Jiang, X. Sun and B. Tang, *Small*, 2024, **20**, 2400141.

4 J. Zhu, J. Chi, T. Cui, L. Guo, S. Wu, B. Li, J. Lai and L. Wang, *Appl. Catal., B*, 2023, **328**, 122487.

5 Y. Pan, Z. Wang, K. Wang, Q. Ye, B. Shen, F. Yang and Y. Cheng, *Adv. Funct. Mater.*, 2024, **34**, 2402264.

6 Y. Wang, P. Yang, Y. Gong, D. Liu, S. Liu, W. Xiao, Z. Xiao, Z. Li, Z. Wu and L. Wang, *Chem. Eng. J.*, 2023, **468**, 143833.

7 J. Liu, J. Yang, Y. Song, J. Sun, Y. Tian, Q. Chen, X. Zhang and L. Zhang, *J. Colloid Interface Sci.*, 2023, **643**, 17−25.

8 K. Wang, X. Liu, Q. Yu, X. Wang, J. Zhu, Y. Li, J. Chi, H. Lin and L. Wang, *Small*, 2024, **20**, 2308613.

9 L. Yu, Q. Zhu, S. Song, B. McElhenny, D. Wang, C. Wu, Z. Qin, J. Bao, Y. Yu, S. Chen and Z. Ren, *Nat. Commun.*, 2019, **10**, 5106.

10 S. Qin, Z. Zhao, J. Sun, Z. Zhang and X. Meng, *Nano Energy*, 2024, **128**, 109921.

11 C. Yang, K. Dong, L. Zhang, X. He, J. Chen, S. Sun, M. Yue, H. Zhang, M. Zhang, D. Zheng, Y. Luo, B. Ying, Q. Liu, A. M. Asiri, M. S. Hamdy and X. Sun, *Inorg. Chem.*, 2023, **62**, 7976−7981.

12 L. Wu, L. Yu, F. Zhang, B. McElhenny, D. Luo, A. Karim, S. Chen and Z. Ren, *Adv. Funct. Mater.* 2021, **31**, 2006484.

13 F. Luo, P. Yu, J. Xiang, J. Jiang and S. Chen, *J. Energy Chem.*, 2024, **94**, 508−516.

14 L. Yu, L. Wu, B. McElhenny, S. Song, D. Luo, F. Zhang, Y. Yu, S. Chen and Z. Ren, *Energy Environ. Sci.*, 2020, **13**, 3439−3446.

15 T. Cui, X. Zhai, L. Guo, J. Q. Chi, Y. Zhang, J. Zhu, X. Sun and L. Wang, *Chin. J. Catal.*, 2022, **43**, 2202−2211.